Received: 17 July 2023 | Revised: 16 November 2023 | Accepted: 2 December 2023

DOI: 10.1111/efp.12842

Forest Pathology WILEY-BLACKWELL WILEY

ORIGINAL ARTICLE

Anatomical and physiological consequences of beech leaf disease in *Fagus grandifolia* L.

Leila R. Fletcher[1] | Aleca M. Borsuk[1] | Ana C. Fanton[2] | Kate M. Johnson[3,4] | Jennifer Richburg[1] | Joseph Zailaa[1] | Craig R. Brodersen[1]

[1]Yale University School of the Environment, New Haven, Connecticut, USA

[2]Ecophysiologie et Génomique Fonctionnelle de la Vigne, INRAE, Villenave-d'Ornon, France

[3]Plant Ecology Research Laboratory PERL, Ecole Polytechnique Fédérale de Lausanne EPFL, Lausanne, Switzerland

[4]Swiss Federal Institute for Forest, Snow and Landscape Research WSL, Birmensdorf, Switzerland

Correspondence
Leila R. Fletcher, Yale University School of the Environment, 370 Prospect Street, New Haven, CT 06511, USA.
Email: leila.fletcher@yale.edu

Funding information
Newman Family Fund for Plant Research

Abstract

Beech leaf disease (BLD) is a foliar disease of American Beech (*Fagus grandifolia* L.) causally linked to the nematode *Litylenchus crenatae mccannii* and has rapidly spread throughout central and northeastern North America. This study aimed to characterize the anatomical and physiological differences between asymptomatic and symptomatic leaves to provide evidence for a mechanistic link between abnormal leaf development associated with BLD and the long-term decline of affected trees. We found that leaf mass per area (LMA) and leaf thickness were 45% and 249% higher in symptomatic regions, respectively. The difference in leaf thickness was largely attributable to the spongy mesophyll being 410% thicker in symptomatic as compared with asymptomatic regions of the leaves, but palisade mesophyll and abaxial epidermal tissues were also thicker in symptomatic regions. While major vein density was not significantly different, minor vein density was significantly lower in symptomatic regions, suggesting that the effects on leaf development occur after the formation and initial development of first- and second-order veins. Stomatal density was also lower in symptomatic leaves. Maximum photosynthetic rates were approximately 61% lower in symptomatic leaves and respiration rate increased as the percentage of affected leaf tissue increased. Collectively, our data show reduced photosynthetic capacity, increased respiration rates, and higher leaf construction costs, which will likely have a negative, long-term impact on the carbon balance of trees affected by BLD.

KEYWORDS
beech leaf disease, *Fagus grandifolia*, leaf anatomy, leaf hydraulics, nematode, photosynthesis, physiology

1 | INTRODUCTION

Beech leaf disease (BLD) affects leaves of American beech (*Fagus grandifolia* L.) and other congeneric species and is causally linked to the foliar nematode *Litylenchus crenatae mccannii* (Carta et al., 2020). Since its first documentation in 2012 in the midwestern United States, BLD spread rapidly eastward throughout the northeastern United States and Canada (Cleveland Metroparks, 2023; Ewing et al., 2019; Marra & LaMondia, 2020; Volk et al., 2019). Recent evidence suggests that while other foliar pathogens and diseases may co-occur with BLD symptoms (Carta et al., 2023; Ewing et al., 2021), the presence of *L. c. mccannii* in developing leaf buds is associated with key BLD symptoms, including abnormal leaf development, necrotic lesions, and ultimately tree mortality (Carta

et al., 2023; Department of Environmental Conservation, 2022; Volk et al., 2019). Typical symptoms of BLD affected trees include the production of leaves with dark green interveinal banding between secondary veins, accompanied variably by chlorosis, necrosis, puckering, and crinkling of the leaf (Carta et al., 2020, 2023). Nematodes can be found in developing leaf buds during late summer, and leaves emerging from these buds the following spring present BLD symptoms (Fearer et al., 2022; Reed et al., 2020; Volk et al., 2019).

To date, no studies have documented the effect of BLD on the leaf vascular system or the link between physiological performance and changes in tissue- and cellular-level anatomy due to BLD. Only one study has investigated the tissue- and cellular-level differences throughout the development of symptomatic and asymptomatic leaves (Vieira et al., 2023), and one other investigated the relationship between symptom severity and physiology (McIntire, 2023). Thus, establishing how anatomical and mechanistic changes caused by *L. crenatae mccannii* result in a decline in tree health is important for understanding the short- and long-term implications of BLD in temperate in forests home to *F. grandifolia*.

The goals of this study were to make anatomical comparisons between symptomatic and asymptomatic leaves from trees in the same population and then to make comparisons with asymptomatic leaves from an isolated population of *F. grandifolia* with no reported BLD-affected trees. We further aimed to characterize the hydraulic and photosynthetic properties of symptomatic and asymptomatic leaves, thereby providing insight into the link between abnormal leaf development and leaf-level physiology. Two sites in Connecticut were selected for our study, one with a mix of symptomatic and asymptomatic leaves (West Rock Ridge State Park in New Haven, CT) with confirmed, PCR-positive tests for the nematode in symptomatic leaves at the same location in 2020 (Dr. Robert Marra, CT Agricultural Experiment Station, personal communication), and a population in northeastern Connecticut (Yale Myers Forest, Union, CT) with only asymptomatic trees (determined by the lack of visual BLD symptoms as no PCR tests were performed at this site). The two sites were approximately 120 km apart, which presented differences in site characteristics that undoubtedly affect tree growth and vigour. To the best of our knowledge, at the time of our sampling, the Yale Myers site was the closest location with a stand of completely asymptomatic trees. Symptomatic leaves have been observed at West Rock Ridge State Park since at least 2020, allowing us to characterize the anatomy and physiology of a stand that has had BLD-affected trees for at least two years and make a direct comparison to trees from an asymptomatic stand.

2 | MATERIALS AND METHODS

2.1 | Sampling

Leaves used for anatomical and leaf hydraulic conductivity measurements were collected from symptomatic and asymptomatic *F. grandifolia* trees at two different sites. One to two branches, approximately 1 meter in length, were collected from eight individuals with both symptomatic and asymptomatic leaves on each branch at West Rock Ridge State Park, New Haven, CT, USA (WR), and from eight asymptomatic trees at Yale Myers Forest, Union, CT, USA (YM) between June and August 2022. Branches were south-facing and approximately 2–3 m above the forest floor from trees 5–20 cm diameter at breast height (1.3 m) at both sites. The collected branches were placed in plastic bags with the cut ends wrapped in wet paper towels. After all sampling trips, branches were brought to the Greeley Memorial Laboratory at Yale University (New Haven, CT, USA) where they were recut under water at least two nodes above the initial cut, covered in dark plastic bags and allowed to rehydrate overnight. Photosynthetic gas-exchange measurements were conducted on trees from the same two sites on leaves from branches still attached to the trees. Traits were divided into four sampling groups: asymptomatic leaves from Yale Myers (YMa), asymptomatic leaves from West Rock (WRa), symptomatic leaves from West Rock (WRs), and for venation traits as described below, asymptomatic sections of symptomatic leaves from West Rock (WRs-a).

2.2 | Measurement of leaf structural traits

Leaf mass per area (LMA), leaf dry matter content (LDMC) and saturated water content (SWC) were measured on each of five asymptomatic leaves per individual for three YMa individuals, and for one asymptomatic leaf each from three WRa individuals, and one to two symptomatic leaves from six WRs individuals. Leaves from both sites were excised from branches that had been rehydrated overnight, as described above, prior to measurement of leaf area. Leaves were then placed in paper envelopes, put in a drying oven at 70°C for at least 3 days, and then weighed (Sartorius PRACTUM224-1S, Goettingen, Germany). LMA was calculated as leaf dry mass (g) divided by leaf area (m^2). LDMC was calculated as leaf dry mass (g) divided by fresh leaf mass (g). Saturated water content was calculated as leaf fresh mass (g) minus leaf dry mass (g), all divided by leaf dry mass (g). For symptomatic leaves, the symptomatic area was manually traced on the leaf scans using ImageJ (version 1.53 k, National Institutes of Health, Bethesda, Maryland, USA). The leaves in our study exhibited banded-type symptoms with some curling or crinkling. We measured the area of all symptomatic regions (banded or crinkled) visible in the scan that contributed to the total symptomatic area. The percent symptomatic area of each leaf was then calculated as symptomatic leaf area divided by total leaf area, all multiplied by 100.

2.3 | Measurement of leaf thickness

Leaf sections were cut using a microtome (Reichert Wien, Eric Sobotka Company) fitted with a freezing stage (BFS-MP Freezing Stage, Physitemp Instruments LLC, Clifton, NJ, USA), and then double stained with a 1:1 blend of safranin (1% in water; Safranin

O 0574-25G, VWR International, LLC, Solon, OH, USA) and astra blue (0.5% in water with 0.2% acetic acid), and mounted in water on glass microscope slides. Transverse sections were imaged on a Canon EOS 6D digital camera connected to an Olympus BX43 (Olympus America) compound light microscope. Leaf thickness, upper and lower epidermal thickness, palisade and spongy mesophyll thickness, and second-order vascular bundle diameter were measured from the images in the FIJI implementation of ImageJ. Traits were measured three times per leaf using one to three leaves per tree. Measurements were replicated for three YMa individuals and for eight WRa and WRs individuals. WR measurements were made on asymptomatic and symptomatic leaves from the same individual.

2.4 | Quantification of leaf venation

Leaves were preserved in 70% formalin-acetic-acid (FAA; 48% ethanol: 10% formalin: 5% glacial acetic acid: 37% water). Three leaves from YMa and seven leaves each from WRa and WRs were used. One leaf per individual was then cleared using 5% sodium hydroxide (NaOH 7708-05, Mallinckrodt, Dublin, Ireland) in water (Scoffoni et al., 2013). The leaves were then further cleared with sodium hypochlorite bleach. Following the clearing, leaves were brought into ethanol (EtOH) solution using a series of dilutions, and then stained with 1% safranin (Safranin O 0574-25G, VWR International, LLC, Solon, OH, USA) and 1% fast green (Fast Green FCF F99-10, Fisher, Fair Lawn, NJ, USA). Using reverse dilutions, leaves were brought back into water and mounted between clear plastic sheets (3M Transparency Film, Austin, TX, USA) for imaging. Whole leaves were scanned (CanoScan LiDE220, Canon Inc.) at 300–1200dpi, and then symptomatic and asymptomatic sections of each leaf were photographed using a light microscope at the base, middle and tip of the leaf (Canon EOS 6D digital camera connected to an Olympus BX43 light microscope, Olympus America). If symptomatic or asymptomatic portions were not present in one of those zones, the image was taken from another zone.

Scanned images were measured for leaf area, perimeter and width. The width of the midrib was measured at the base, middle and tip of the leaf, and the length of the midrib was also measured. The widths of three secondary veins located at the base, middle and tip of the leaf were each measured twice, once near the center and once near the margin of the leaf, for a total of six measurements per leaf. The lengths of all secondary veins were measured on each leaf and then summed to obtain total secondary vein length (except in two cases where one side of the leaf was damaged and would not allow for accurate measurements, and thus all secondaries on one half of the leaf were measured instead, and these measurements were doubled in the calculation of secondary vein length). The length of all tertiary veins was measured in three 112 mm^2 areas at the base, middle and tip of each leaf. In the case of symptomatic leaves, this technique was used to measure tertiaries in both asymptomatic and symptomatic regions of the leaf.

The widths of the tertiary and minor veins were measured on the microscope images, with two measurements being made on images from each of the base, middle and tip of the leaves (for a total of six measurements per trait). The length of all the minor veins in a ~3 mm^2 area was measured and summed for regions at the base, middle and tip of each leaf. For symptomatic leaves, this was repeated on both asymptomatic and symptomatic portions of each leaf.

The vein length per area (VLA) was then calculated for every vein order as vein length divided by area of the leaf or measured region. Additionally, the projected vein area per leaf area (APA) was calculated as the sum of the width multiplied by the VLA of each vein order (Sack et al., 2012). The volume of leaf vein per leaf area (VPA) was calculated as the sum of the VLA multiplied by π and the radius^2 of each vein order, where the radius was estimated as vein width divided by two (Sack et al., 2012). For leaves that showed symptoms, APA and VPA were calculated twice–once using the lengths and widths from asymptomatic portions of the leaves, and once using lengths and widths from symptomatic portions of the leaves in order to compare what these values would be if all tertiary and minor veins were either asymptomatic or symptomatic.

2.5 | Quantification of stomatal traits

Fresh leaves were used for the quantification of stomatal traits. Clear nail polish (Sally Hansen, Coty, NY, USA) was applied to the abaxial surfaces of the leaves, peeled off and placed onto slides, which were imaged using a light microscope (as above). Stomatal density (SD) was measured on 8–13 leaves per group on both the full image area and on the image area minus the vein area. Guard cell length and width, and inner and outer pore lengths were measured on four stomata per image.

2.6 | Gas exchange measurements

To determine the effect of BLD on leaf photosynthetic capacity light response curves were generated using a portable gas-exchange system on at least six leaves per group (LI-6800, Licor Inc.). Measurements were made between 9:30am and 3pm on 03 August 2022 for leaves from YM, and on 18 August 2022 for leaves from WR, both of which were sunny days. Leaves were placed in the gas-exchange cuvette so that they filled the 3×3 cm cuvette and were allowed to acclimate at 500 $\mu mol\, m^{-2} s^{-1}$ PPFD for 5min. Leaves then progressed through a series of declining light intensity values (1500, 1000, 750, 500, 250, 100, 50, 0 $\mu mol\, m^{-2} s^{-1}$ PPFD) after reaching a stability value of 5% coefficient of variation. Steady conditions within the cuvette were maintained at 60% relative humidity with a carbon dioxide concentration of 400 $\mu mol\, m^{-1}$ and with temperature controls matching ambient conditions. The asymptomatic and symptomatic leaf tissue area within the cuvette was calculated by scanning and measuring the leaves after the completion of the light response curves.

2.7 | Leaf hydraulic measurements

Measurements of leaf hydraulic conductance were made using the evaporative flux method (Sack & Scoffoni, 2012) using 18 WRa leaves, 19 WRs leaves, and 13 YMa leaves. Smaller segments containing at least three leaves were cut from the rehydrated branches and put into plastic bags to equilibrate for at least 20 min. The middle leaf was cut under deionized water, and the petiole was wrapped in parafilm and connected to tubing. The tubing led to a water source (degassed Millipore water, Millipore Milli-Q Water Purification System, Darmstadt, Germany) on a balance (Sartorius PRACTUM224-1S, Goettingen, Germany), which logged the flow rate of water into the leaf every 10 s (WinWedge v3.4.3 Standard Edition, TAL Technologies, Philadelphia, PA, USA). The leaf was placed over a box fan and under a light with an intensity of >1000 μmol m^{-2} s^{-1} (LumiGrow PRO 325, Emeryville, CA, USA, used for light, intensity measured with Li-Cor Light Meter Model LI-189, Lincoln, NE, USA). Leaf temperature was maintained below 30°C (monitored with FLUKE-62 MAX IR Thermometer, Everett, WA, USA). Leaves were left on the system for at least 20 min or until the flow rate stabilized, whichever was longer. A stable flow rate was defined by the coefficient of variation <5% over the course of the 5-min period before the measurement was recorded. Once a stable flow rate was achieved, the leaf temperature was recorded and the leaf was removed from the system and scanned for leaf area (CanoScan LiDE220, Canon Inc.). The leaf was then placed into a plastic bag into which the experimenter had previously exhaled, then into another bag containing wet paper towels, and allowed to sit for at least 30 min for equilibration to increase relative humidity and ensure stomatal closure. Once equilibrated, the final leaf water potential (Ψ_{final}) was measured using a pressure chamber (PMS Instrument Co. Model 1505D Pressure Chamber Instrument, Albany, OR, USA) with the grass compression gland insert. Immediately after the excision of the middle leaf that was used for hydraulic measurements, the leaves adjacent on the branch were also measured for an initial leaf water potential ($\Psi_{initial}$) using the pressure chamber. Only values of K_{leaf} for which the lowest Ψ_{leaf} was between −0.3 and −0.8 were included in the analysis to standardize comparisons across dehydration levels. A Dixon's outlier test was performed on K_{leaf} data in this range, and one outlier point was removed.

2.8 | Statistical analyses

All statistical analyses were performed in the R Statistics environment (R version 4.0.5). Analyses of variance (ANOVAs) were performed to test for variation among groups—asymptomatic leaves from YM site (YMa), asymptomatic leaves from WR site (WRa), symptomatic leaves from WR site (WRs), and when appropriate, asymptomatic sections of symptomatic leaves from WR site (WRs-a)—using the *aov* and *anova* functions in the stats package. For traits for which the ANOVA results were significant, the Tukey's Honest Significant Difference post-hoc method was performed using the *TukeyHSD* function in the stats package to determine which specific groups were significantly different from each other. Linear correlations between several traits and the percent of symptomatic leaf area were tested using the *lm* function in the stats package.

3 | RESULTS

3.1 | Leaf anatomical trait variation

We observed a range of symptom severity at the WR site (Figure 1), including both symptomatic and asymptomatic leaves on the same branches, and symptomatic leaves with varying degrees of affected leaf area (10%–93% of the leaf area showing symptoms, with mean of 49% in our samples). There were statistically significant differences in anatomy between asymptomatic and symptomatic leaf tissue, and there was limited variation between asymptomatic leaves at the two study sites (Table 1). LMA and SWC were 45% and 25% higher in symptomatic leaves, respectively, while LDMC was 12% lower in symptomatic leaves than in asymptomatic leaves (Table 1; Table S1). We found a positive, linear relationship between the percentage of symptomatic leaf area and LMA ($r = 0.78$, $p < .001$; Figure 2a; Table S2).

FIGURE 1 Representative *Fagus grandifolia* leaves from West Rock Ridge State Park with increasing percentage of symptomatic area. Leaves span the range from asymptomatic to almost completely affected by banded or crinkled-type beech leaf disease (BLD) symptoms.

TABLE 1 Traits measured for beech (*Fagus grandifolia*) leaves collected from two field sites (Yale Myers, YM and West Rock, WR) with the following leaf conditions: asymptomatic (WRa, YMa), symptomatic (WRs), asymptomatic portions of symptomatic leaves (WRs-a). Variation across groups is presented in the form of group means, along with mean squares (MS), the proportion of variance explained by difference between groups (PoV; the remainder being explained within groups), degrees of freedom (df), and *F*- and *p*-values from analyses of variance (ANOVA). Significance levels for ANOVA results are as follows: ns; $p > .05$; $^{*}p < .05$; $^{**}p < .01$; $^{***}p < .001$.

Trait	Units	Group means (YMa, WRa, WRs, WRs-a if applicable)	ANOVA			
			MS, PoV	df1, df2	*F*-value	*p*-value
Structural traits						
Leaf mass per area (LMA)	$g\,m^{-2}$	29.6, 29.0, 42.4	983.82, 0.44	2, 57	22.145	7.65e-08***[a]
Leaf dry matter content (LDMC)	$g\,g^{-1}$	0.424, 0.418, 0.368	1.5424e-2, 0.57	2, 57	37.524	4.00e-11***[a]
Saturated water content (SWC)	$g\,g^{-1}$	1.36, 1.40, 1.74	0.70179, 0.57	2, 57	37.988	3.27e-11***[a]
Anatomical traits						
Leaf thickness (LT)	mm	78.0, 78.9, 274	88,547, 0.92	2, 16	98.655	1.00e-09***[a]
Adaxial epidermal thickness (AD)	mm	9.63, 8.94, 17.8	174.27, 0.49	2, 16	7.5946	4.80e-03**[b]
Abaxial epidermal thickness (AB)	mm	7.27, 7.67, 21.0	418.26, 0.69	2, 16	17.518	9.33e-05***[a]
Palisade mesophyll thickness (PM)	mm	22.7, 24.6, 41.3	689.80, 0.53	2, 16	9.0947	2.30e-03**[a]
Spongy mesophyll thickness (SM)	mm	36.5, 36.6, 187	52,104, 0.96	2, 16	185.49	8.54e-12***[a]
Vein traits						
Midrib vein length per area (VLA)	$mm\,mm^{-2}$	2.23e-2, 2.64e-2, 2.54e-2	1.7905e-5, 0.07	2, 14	0.5369	5.96e-01
Secondary vein length per area (VLA)	$mm\,mm^{-2}$	0.151, 0.175, 0.180	9.1799e-4, 0.18	2, 14	1.5236	2.52e-01
Tertiary vein length per area (VLA)	$mm\,mm^{-2}$	0.561, 0.583, 0.607, 0.643	6.4474e-3, 0.10	3, 20	0.7777	5.20e-01
Minor vein length per area (VLA)	$mm\,mm^{-2}$	7.65, 8.09, 5.89, 8.68	10.039, 0.63	3, 20	11.588	1.28e-04***[b]
Midrib width	mm	0.275, 0.365, 0.418	2.1543e-2, 0.13	2, 14	1.0855	3.65e-01
Secondary vein width	mm	0.183, 0.147, 0.160	1.3982e-3, 0.23	2, 14	2.1321	1.56e-01
Tertiary vein width	mm	5.08e-2, 4.72e-2, 7.48e-2, 5.16e-2	1.0681e-3, 0.79	3, 20	24.642	6.37e-07***[a]
Minor vein width	mm	2.32e-2, 2.11e-2, 4.42e-2, 2.37e-2	7.8232e-4, 0.89	3, 20	53.518	9.76e-10***[a]
Projected vein area per area (APA)	$mm^2\,mm^{-2}$	0.239, 0.233, 0.386, 0.274	3.20e-2, 0.74	3, 20	19.162	4.25e-06***[a]
Volume of veins per area (VPA)	$mm^3\,mm^{-2}$	9.85e-3, 9.61e-3, 2.01e-2, 1.30e-2	1.50e-4, 0.51	3, 20	7.0527	2.03e-03**[a]
Stomatal traits						
Stomatal density (SD)	$n\,\mu m^{-2}$	295, 284, 158	65,908, 0.49	2, 28	13.386	8.33e-05***[a]
Stomatal density with veins	$n\,\mu m^{-2}$	270, 267, 135	67,479, 0.61	2, 28	21.455	2.24e-06***[a]
Stomatal length (SL)	mm	15.8, 15.1, 20.6	404.79, 0.55	2, 121	73.21	2.20e-16***[a]
Stomatal width (SW)	mm	18.4, 17, 20.6	134.25, 0.38	2, 121	37.811	1.75e-13***[c]
Physiological traits						
Maximum photosynthetic rate (A_{1000})	$\mu mol\,m^{-2}\,s^{-1}$	5.50, 5.28, 2.12	24.273, 0.53	2, 16	9.1763	2.22e-03**[a]
Maximum stomatal conductance (g_{s1000})	$mmol\,m^{-2}\,s^{-1}$	80.7, 66.2, 24.8	6.0487e-3, 0.55	2, 16	9.7075	1.74e-03**[a]
Dark respiration rate (R_{dark})	$\mu mol\,m^{-2}\,s^{-1}$	−0.356, −0.159, −0.494	0.14328, 0.34	2, 16	4.0489	3.78e-02*[b]
Leaf hydraulic conductance (K_{leaf})	$mmol\,m^{-2}\,s^{-1}\,MPa^{-1}$	1.27, 1.28, 1.56	0.33254, 0.15	2, 29	2.4592	1.03e-01

[a]WRs was significantly different from WRa and YMa (and WRs-a, if applicable), but asymptomatic groups were not significantly different from each other.

[b]WRs was significantly different from WRa (and WRs-a if applicable), but not from YMa, and asymptomatic groups were not significantly different from each other.

[c]All groups were significantly different from each other.

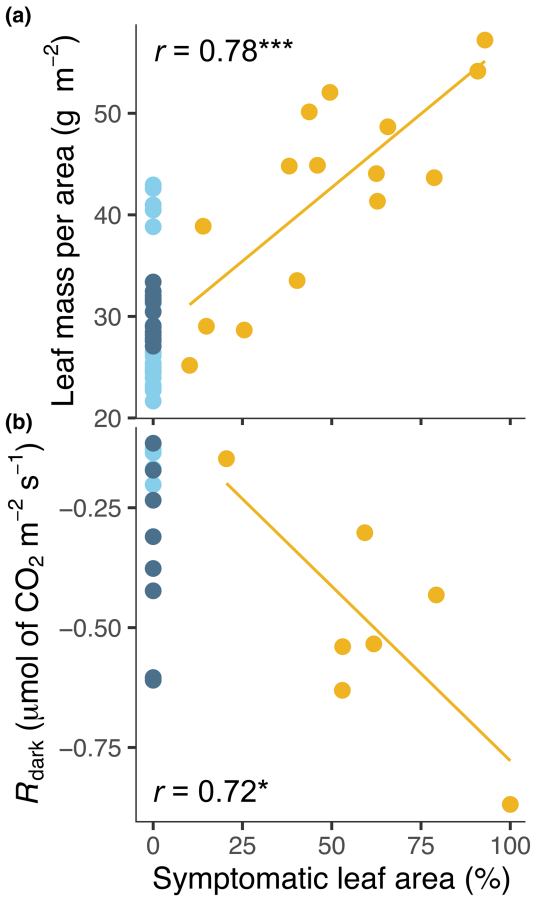

FIGURE 2 Relationships of (a) leaf mass per area and (b) dark respiration rate with the percentage of symptomatic leaf area for leaves from *Fagus grandifolia* sampled from two sites and different leaf conditions; asymptomatic leaves from Yale Myers Forest (dark blue); asymptomatic leaves from West Rock (light blue); symptomatic leaves from West Rock (yellow). The *r*-value with significance is from linear regression, $^{*}p < .05$; $^{***}p < .001$.

Transverse cross sections through leaves revealed that total leaf thickness was significantly higher in symptomatic regions as compared to asymptomatic regions (Figure 3a,b). Differences in total leaf thickness were primarily due to a 410% higher spongy mesophyll thickness, but we also found that the symptomatic regions had a 72% thicker palisade layer and 178% thicker abaxial epidermis (Figure 3b, Table 1; Table S3). Asymptomatic cell layers from both the isolated YM population and the WR site were not significantly different (Table 1, Figure 3c).

We found striking differences in leaf vein density (mm vein length/mm^2 leaf area) and vein width between adjacent symptomatic and asymptomatic regions of BLD-affected leaves (Figure 4a), but the differences were vein order-dependent. First- (midvein), second- and third-order VLA were not significantly different, but minor VLA was 29% lower in symptomatic regions (Table 1, Figure 4a,b; Table S4). Minor VLA did not differ significantly between asymptomatic groups, but was significantly lower in WRs leaves as compared with WRa and WRs-a leaves. However, minor VLA in WRs leaves was lower, but not significantly different from that of leaves in the YM site despite the confidence intervals of those groups not overlapping ($p = .058$; Table 1, Figure 4b). Tertiary and minor veins were 51 and 96% wider in symptomatic regions (Figure 4b, Table S4), but there were no significant differences in the widths of first- and second-order veins between symptomatic and asymptomatic leaves. APA and VPA were 54 and 82% higher in symptomatic tissue, respectively (Table 1).

Finally, stomatal density (SD) was 46%–50% lower in symptomatic tissue when excluding or including vein area in the calculations, respectively (Table S5). SD was also highly variable in symptomatic tissue. In some symptomatic regions we found SD to be over 69% lower than asymptomatic regions of the same leaf, while in other symptomatic leaves SD was as high as 378 mm^{-2} (Figure 5c). Similarly, guard cell length was 33% higher in symptomatic regions, while guard cell width varied between groups and sites (Table 1; Table S5).

3.2 | Physiological variation

Maximum photosynthetic rate and stomatal conductance were 61% and 67% lower in symptomatic leaves (Figure 5a,b), while the asymptomatic leaves at the two sites were not significantly different (Table S6). WR leaves had less negative dark respiration rates than both WRs and YMa leaves (Table 1). However, WRs leaves still had the most negative dark respiration rates. Dark respiration rate also became more negative with a higher percentage of symptomatic leaf area ($r = 0.72$, $p < .05$; Figure 2b; Table S2). Leaf hydraulic conductance (K_{leaf}) did not differ based on leaf condition or collection site (Table 1; Figure 5d; Table S7). Maximum photosynthetic rate and stomatal conductance did not show a significant trend with percentage of symptomatic leaf area, nor did K_{leaf} (Table S2).

4 | DISCUSSION

4.1 | Anatomical impacts of BLD

Our anatomical characterization of BLD-affected leaves is consistent with previous reports of spatially explicit symptoms in American beech leaves in response to the foliar nematode *L. crenatae mccannii* (Carta et al., 2023; Cleveland Metroparks, 2023; Ewing et al., 2019; Marra & LaMondia, 2020; Vieira et al., 2023; Volk et al., 2019). Notably, the dark green banding between second-order veins can now be attributed to increased leaf thickness resulting from additional chlorophyll-containing mesophyll cell layers and abnormal development of the spongy mesophyll. This is consistent with previous work showing that nitrogen content increases with symptom severity (McIntire, 2023), and that chloroplast content is higher in symptomatic leaves (Vieira et al., 2023). Leaf clearing revealed the reduced density of third-order veins,

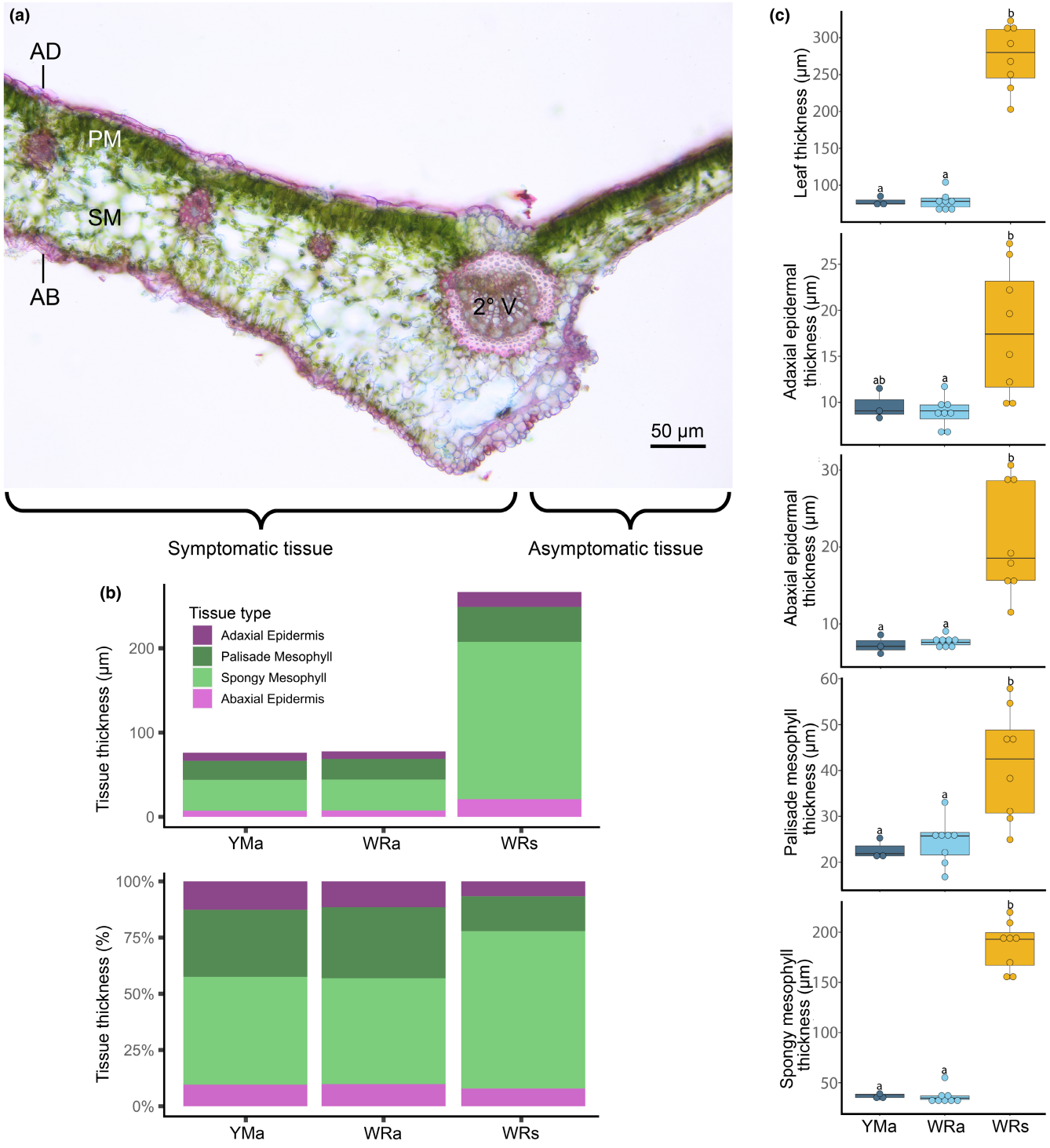

FIGURE 3 Anatomical traits measured from transverse sections of the leaf lamina for *Fagus grandifolia* sampled from two sites and different leaf conditions. (a) Transverse section of a representative symptomatic leaf with asymptomatic and symptomatic tissue on either side of a secondary vein; AB, abaxial epidermis; AD, adaxial epidermis; PM, palisade mesophyll tissue; SM, spongy mesophyll tissue; 2° V, secondary vein. (b) Absolute and proportional leaf tissue thicknesses for asymptomatic and symptomatic leaves. (c) Standard boxplots showing variation in tissue thicknesses across sites; YMa, asymptomatic leaves from Yale Myers Forest; WRa, asymptomatic leaves from West Rock; WRs, symptomatic leaves from West Rock. The black line indicates the median and the whiskers indicate points up to 1.5 times outside the interquartile range. Letters above the boxes indicate significant differences between groups from a Tukey's Honest Significant Differences test.

thicker veins in general, and an effective absence of higher order veins. Because the first- (midvein) and second-order veins appear to develop normally, we conclude that the disease may disrupt cellular divisions at the later stages of leaf development where there may be coordination between higher order vein development and stomatal patterning (Zhang et al., 2022).

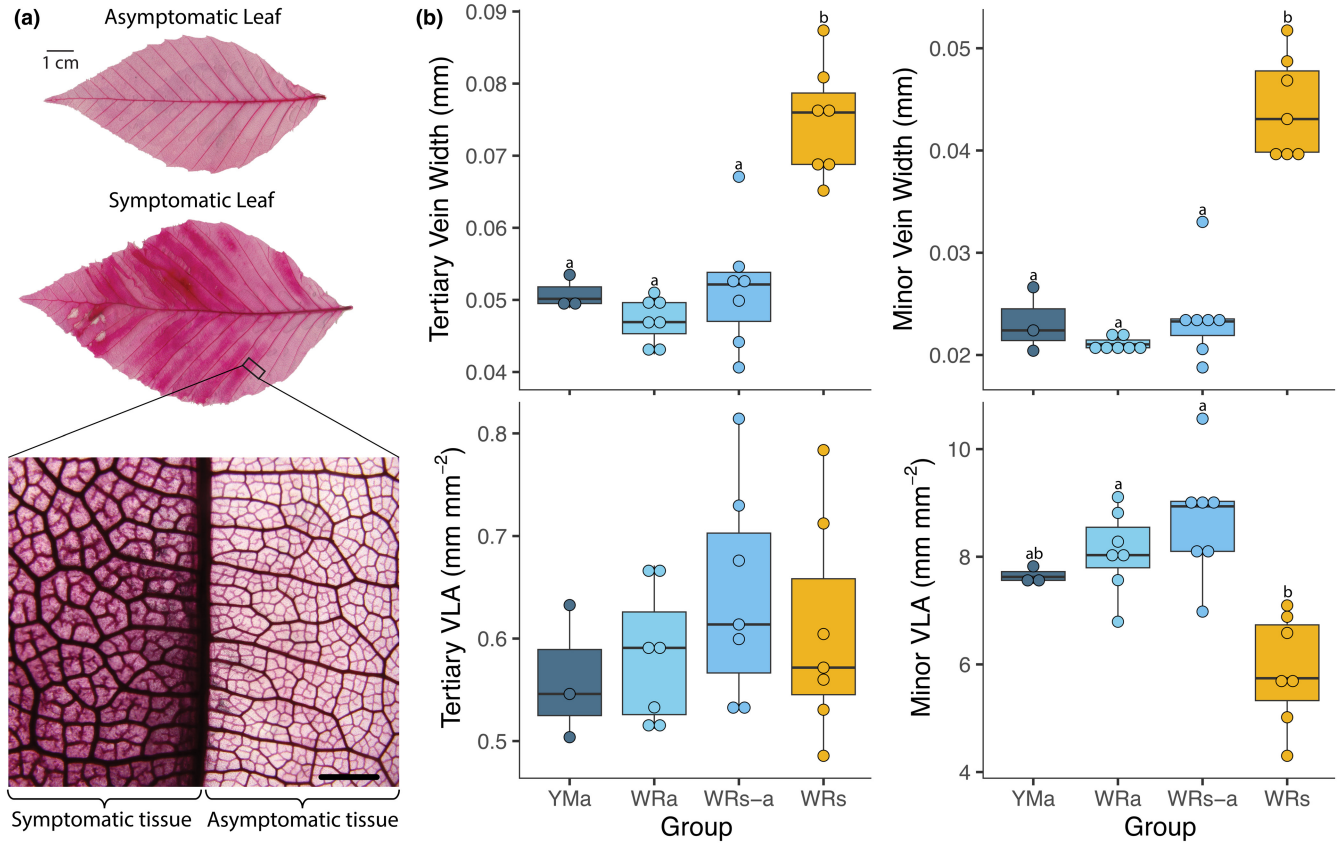

FIGURE 4 Vein density variation in symptomatic and asymptomatic *Fagus grandifolia* leaves from two sites and different leaf conditions. (a) Examples of asymptomatic and symptomatic leaves that have been chemically cleared and stained for visualization of the major veins. Whole leaf images come from scans and the close-up is a microscope image of a symptomatic leaf from West Rock with a secondary vein running through the center. Asymptomatic tissue is on the right side and symptomatic tissue is on the left, scalebar = 1 mm. (b) Standard boxplots showing variation in vein width and vein length per area (VLA) for different vein orders across sites and leaf conditions. YMa, asymptomatic leaves from Yale Myers Forest; WRa, asymptomatic leaves from West Rock; WRs, symptomatic leaves from West Rock; WRs-a, asymptomatic portions of symptomatic leaves from West Rock. The black line indicates the median and the whiskers indicate points up to 1.5 times outside the interquartile range. Letters above the boxes indicate significant differences between groups from a Tukey's Honest Significant Differences test.

4.2 | Relationships between anatomical, hydraulic and photosynthetic traits

Regarding leaf physiology, we observed reduced photosynthetic rates in BLD-affected leaves without a significant decline in leaf hydraulic conductance. This was surprising, given water availability is crucial for optimizing photosynthetic productivity, where water lost during transpiration must be replaced by the leaf vein network (Boyce et al., 2009; Brodribb et al., 2005, 2007; Sack et al., 2003, 2013; Sack & Scoffoni, 2013; Sack & Tyree, 2005). Our results point to several possible explanations. First, we expected that the reduced vein density of symptomatic leaves would lead to reduced K_{leaf}, as water would have to travel greater distances from the vein endings to the points of evaporation inside the leaf. Reduced stomatal density would further compound this effect, thereby significantly increasing the total hydraulic resistance of the leaf. Such a relationship would then logically lead to the observed reduced photosynthetic rates (Figure 5a). However, K_{leaf} was not significantly lower in symptomatic leaves. One possible explanation is that lower minor vein density was offset by increased vein width in symptomatic leaves, where increased conduit number or increased conduit radius would lead to higher transport rates (Tyree & Ewers, 1991). Another explanation could be linked to increased projected vein area per leaf area (APA). Symptomatic leaves from WR had higher APA than asymptomatic leaves from either site, with wider veins occupying a larger fraction of the overall leaf surface (Table 1). Thus, wider veins reduce the total leaf area that can be occupied by photosynthetic cells. Another explanation may arise from differences in the anatomical structure of symptomatic leaves. While symptomatic regions were thicker, spongy mesophyll porosity also appeared to be much higher. The increased airspace volume would increase the diffusive pathway for both water vapour and CO_2 inside the leaf. Thus, the greater distance that CO_2 must travel from the stomatal openings in the abaxial epidermis to the palisade layer may reduce overall mesophyll conductance, thereby limiting maximum photosynthetic rates in symptomatic leaves (Gago et al., 2020).

Our data suggest that while there may be some non-stomatal limitations to maximum photosynthetic rates, stomatal limitations

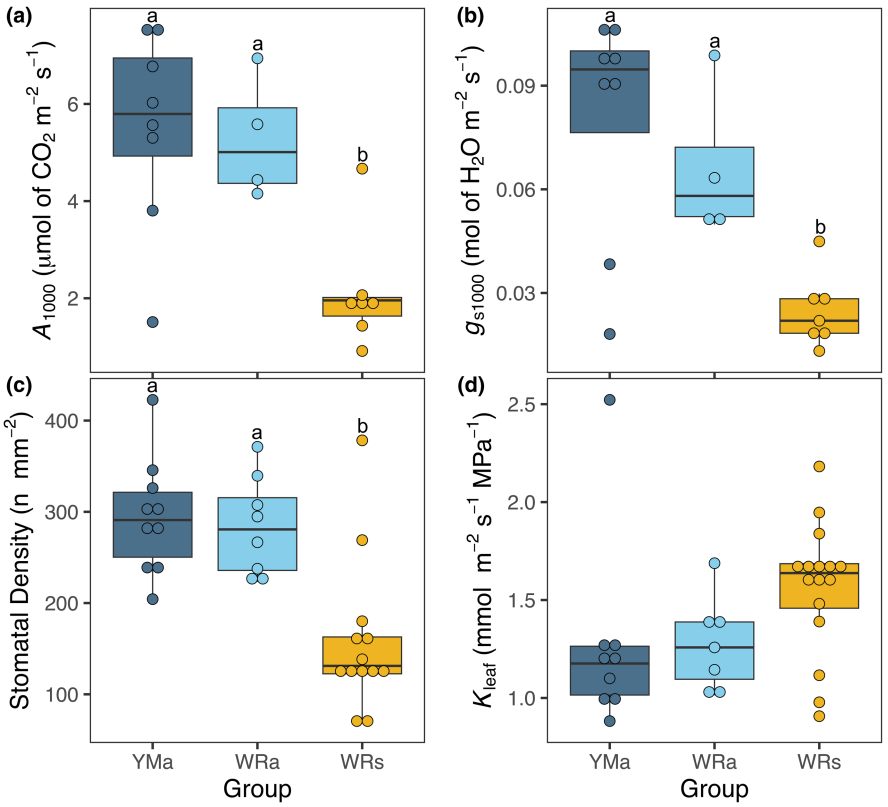

FIGURE 5 Standard boxplots of photosynthetic, hydraulic and stomatal traits for *Fagus grandifolia* leaves from two sites. (a) Photosynthetic rate (A_{1000}) and (b) stomatal conductance (g_{1000}) at 1000 μmol m^{-2} s^{-1} of light, (c) stomatal density not including the area occupied by veins, and (d) leaf hydraulic conductance (K_{leaf}). YMa, asymptomatic leaves from Yale Myers Forest; WRa, asymptomatic leaves from West Rock; WRs, symptomatic leaves from West Rock. The black line indicates the median and the whiskers indicate points up to 1.5 times outside the interquartile range. Letters above the boxes indicate significant differences between groups from a Tukey's Honest Significant Differences test.

may be more or equally influential. Symptomatic regions had lower stomatal density, in some cases up to 69% lower, thereby reducing the overall conductance of the leaf surface to H_2O and CO_2. We attribute the reduced stomatal conductance to the reduced stomatal density in these leaves, which ultimately influences the maximum photosynthetic rate. Recent work by Carta et al. (2023) suggests that stomata in infected leaves are deformed, potentially limiting stomatal control, which could also contribute to the reduced stomatal conductance in symptomatic leaves, although we could not determine this from our stomatal peels. Among symptomatic leaves we found that along with LMA, respiration rate per unit leaf area increased with increasing proportion of diseased leaf area, suggesting that the additional cell layers in symptomatic regions, primarily in the spongy mesophyll, increase the overall operating costs of these leaves from a respiration standpoint. This conclusion is consistent with the findings of McIntire (2023), which found that both LMA (expressed as its inverse, specific leaf area, in that study) and dark respiration rate increased with severity of BLD symptom type.

4.3 | Implications for carbon assimilation capacity

Our findings suggest that BLD has the potential to reduce carbon assimilation capacity in American beech trees. Decreased photosynthetic rates in symptomatic leaves in combination with the increased mass allocation to symptomatic leaf tissue would lead to reduced net carbon gain in the short term, and may cause depletion of the trees' stored carbon and an inability to sustain growth in the long term. Another symptom of BLD is increased bud abortion leading to canopy thinning (Fearer et al., 2022), which in combination with the low photosynthetic rates of the remaining leaves would substantially limit the trees' net carbon gain. This combination may ultimately provide a mechanistic explanation for the observed decline in tree vigour post-infection. Our work affirms and extends another recent finding that photosynthetic rates were lower in symptomatic than asymptomatic leaves of understory beech trees in central Connecticut (McIntire, 2023), thereby suggesting that the physiological effects of BLD are comparable across at least two sites in New England. Additional measurements of reduced photosynthetic rates at more sites will ultimately provide critical information for long-term monitoring and modelling of forest carbon dynamics.

Our results show that the more severely symptomatic an individual leaf is, the more carbon the plant allocates to that leaf. The positive relationship between LMA and the percentage of symptomatic leaf area indicates that the increased leaf thickness in symptomatic tissue is not driven solely by an increase in airspace or water mass, but by a greater biomass investment. This is further supported by the cross-sectional anatomy of the thick, symptomatic leaves, which shows many layers of spongy mesophyll cells and at least two layers of palisade cells. While we did not observe nematodes in our leaf cross-sections, recent scanning electron microscopy has shown that nematodes can be present in symptomatic leaves (Carta et al., 2023), indicating that the greater mass in infected leaves may in part come from nematodes in addition to thicker leaf tissue. However, another recent study found that dark-green banded tissue, which was common in our study, often does not contain nematodes (Vieira et al., 2023).

Based on our observations in the field and previous work (Fearer et al., 2022; Volk et al., 2019), the most severely symptomatic leaves senesce early, meaning that these are shed in favour of growing new leaves. The trigger of this is not known, but with high levels of abscisic acid (ABA) associated with leaf death in diverse land plants (McAdam et al., 2022), the role of hormones such as ABA in triggering early leaf death as a result of BLD should be investigated. In addition to producing more costly high-LMA leaves with low photosynthetic capacity, symptomatic trees may also be investing in at least two leaf cohorts per season (personal observations, personal communication with Dr. Robert Marra, CT Agricultural Experiment Station, Fearer et al., 2022; Volk et al., 2019), which could further contribute to the reduction of their non-structural carbohydrate reserves, eventually leading to mortality. Future work should analyse the non-structural carbohydrate concentrations in symptomatic beech to fully validate this hypothesis. The reduction in carbon has been suggested to limit the ability of ectomycorrhizal fungi to form symbioses with symptomatic beech trees due to the inability of these trees to provide the fungi with sugars in exchange for nutrients, which may further affect the health of infected beech trees (Bashian-Victoroff et al., 2023). BLD may also impact the composition of plant communities and animals reliant on beech leaves and beechnuts, but the ecosystem-level implications of the disease are not yet known (Cale et al., 2017; DeGraaf & Rudis, 1986; Garnas et al., 2011; Jakubas et al., 2005; Jones & Raynal, 1987; Klots & Dospassos, 1981; Lovett et al., 2006, 2010; Martin et al., 1951; Tsai & Manos, 2010).

4.4 | Conclusion

We conclude that BLD, likely in combination with other foliar pathogens and canopy thinning (Fearer et al., 2022), causes a reduction in carbon assimilation capacity, which can potentially lead to tree mortality by depleting the trees' stored carbon. This shortage of resources may arise from the combination of lower photosynthetic rates in symptomatic tissue and higher carbon investment those tissues. A combination of reduced leaf area for photosynthetic tissues, and stomatal limitation due to reduced stomatal density and stomatal deformation likely lead to the reduced photosynthetic rates observed in symptomatic leaves (Carta et al., 2023). While the mechanisms through which the presence of the nematodes leads to abnormal leaf development are unknown, the nematodes' influence appears to be localized both in space and time. First- and second-order veins develop normally, likely while the bud develops in the previous growing season. However, subsequent leaf development is locally affected, reducing minor vein and stomatal densities, and increasing vein width and stomatal size. Interestingly, this only occurs within domains bounded by second-order veins, since asymptomatic tissue in adjacent domains can be observed within the same leaf (Figure 4a). We propose that the presence of the nematode therefore influences the physical or hormonal regulation of leaf development after the development of primary and secondary order veins, within regions bounded by second-order veins. Further investigation of the hormonal signalling that may be disrupted by the nematode during leaf development is therefore of high priority for future work. This study furthers our understanding of how beech trees may decline due to BLD and provides opportunities to use physiological data to predict the large-scale impacts of the disease on the North American deciduous forest ecosystem.

ACKNOWLEDGEMENTS

The authors kindly thank Dr. Robert Marra of the Connecticut Agricultural Experiment Station for initial discussions of the project, selection of study sites, and confirmation of PCR testing results in BLD-affected trees. LRF and CRB were supported by the Newman Family Fund for Plant Research.

CONFLICT OF INTEREST STATEMENT

We have no conflicts of interest to declare.

DATA AVAILABILITY STATEMENT

The data that support the findings of this study are available in the supplementary material of this article.

ORCID

Leila R. Fletcher https://orcid.org/0000-0002-2380-041X
Aleca M. Borsuk https://orcid.org/0000-0002-1696-9647
Ana C. Fanton https://orcid.org/0000-0002-7154-2822
Kate M. Johnson https://orcid.org/0000-0002-3039-6339
Joseph Zailaa https://orcid.org/0000-0001-9103-190X
Craig R. Brodersen https://orcid.org/0000-0002-0924-2570

REFERENCES

Bashian-Victoroff, C., Brown, A., Loyd, A. L., Carrino-Kyker, S. R., & Burke, D. J. (2023). Beech leaf disease severity affects ectomycorrhizal colonization and fungal taxa composition. *Journal of Fungi*, *9*(4), 497. https://doi.org/10.3390/jof9040497

Boyce, C. K., Brodribb, T. J., Feild, T. S., & Zwieniecki, M. A. (2009). Angiosperm leaf vein evolution was physiologically and environmentally transformative. *Proceedings of the Royal Society B-Biological Sciences*, *276*(1663), 1771–1776. https://doi.org/10.1098/rspb.2008.1919

Brodribb, T. J., Feild, T. S., & Jordan, G. J. (2007). Leaf maximum photosynthetic rate and venation are linked by hydraulics. *Plant Physiology*, *144*(4), 1890–1898. https://doi.org/10.1104/pp.107.101352

Brodribb, T. J., Holbrook, N. M., Zwieniecki, M. A., & Palma, B. (2005). Leaf hydraulic capacity in ferns, conifers and angiosperms: Impacts on photosynthetic maxima. *New Phytologist*, *165*(3), 839–846. https://doi.org/10.1111/j.1469-8137.2004.01259.x

Cale, J. A., Garrison-Johnston, M. T., Teale, S. A., & Castello, J. D. (2017). Beech bark disease in North America: Over a century of research revisited. *Forest Ecology and Management*, *394*, 86–103. https://doi.org/10.1016/j.foreco.2017.03.031

Carta, L. K., Handoo, Z. A., Li, S. G., Kantor, M., Bauchan, G., McCann, D., Gabriel, C. K., Yu, Q., Reed, S., Koch, J., Martin, D., & Burke, D. J. (2020). Beech leaf disease symptoms caused by newly recognized nematode subspecies Litylenchus crenatae mccannii (Anguinata) described from *Fagus grandifolia* in North America. *Forest Pathology*, *50*(2), e12580. https://doi.org/10.1111/efp.12580

Carta, L. K., Li, S., & Mowery, J. (2023). Chapter 8—Beech leaf disease (BLD), Litylenchus crenatae and its potential microbial virulence factors. In F. O. Asiegbu & A. Kovalchuk (Eds.), *Forest microbiology*

Vol. 3 (pp. 183–192). Academic Press. https://doi.org/10.1016/B978-0-443-18694-3.00018-3

Cleveland Metroparks. (2023). *BLD map by year*. Cleveland Metroparks, USDA Forest Service https://www.clevelandmetroparks.com/getmedia/ba78fbe2-a196-46a6-bb8b-b4015ea52872/Feb-2023_BLD-by-year-1.png.ashx

DeGraaf, R. M., & Rudis, D. D. (1986). *New England wildlife: Habitat, natural history, and distribution*. https://doi.org/10.2737/NE-GTR-108

Department of Environmental Conservation. (2022). *Beech Leaf Disease*. New York State https://www.dec.ny.gov/lands/120589.html

Ewing, C. J., Hausman, C. E., Pogacnik, J., Slot, J., & Bonello, P. (2019). Beech leaf disease: An emerging forest epidemic. *Forest Pathology*, *49*(2), e12488. https://doi.org/10.1111/efp.12488

Ewing, C. J., Slot, J., Benitez, M. S., Rosa, C., Malacrino, A., Bennett, A., & Bonello, E. (2021). The foliar microbiome suggests that fungal and bacterial agents may be involved in the beech leaf disease Pathosystem. *Phytobiomes Journal*, *5*(3), 335–349. https://doi.org/10.1094/pbiomes-12-20-0088-r

Fearer, C. J., Volk, D., Hausman, C. E., & Bonello, P. (2022). Monitoring foliar symptom expression in beech leaf disease through time. *Forest Pathology*, *52*(1), e12725. https://doi.org/10.1111/efp.12725

Gago, J., Daloso, D. M., Carriquí, M., Nadal, M., Morales, M., Araújo, W. L., Nunes-Nesi, A., & Flexas, J. (2020). Mesophyll conductance: The leaf corridors for photosynthesis. *Biochemical Society Transactions*, *48*(2), 429–439. https://doi.org/10.1042/bst20190312

Garnas, J. R., Ayres, M. P., Liebhold, A. M., & Evans, C. (2011). Subcontinental impacts of an invasive tree disease on forest structure and dynamics. *Journal of Ecology*, *99*(2), 532–541. https://doi.org/10.1111/j.1365-2745.2010.01791.x

Jakubas, W., McLaughlin, C., Jensen, P., & McNulty, S. (2005). *Alternate year beechnut production and its influence on bear and marten populations*. Beech Bark Disease: Proceedings of the Beech Bark Disease Symposium. *General Technical* Report. NE-331.

Jones, R. H., & Raynal, D. J. (1987). Root sprouting in american beech - production, survival, and the effect of parent tree vigor. *Canadian Journal of Forest Research-Revue Canadienne De Recherche Forestiere*, *17*(6), 539–544. https://doi.org/10.1139/x87-090

Klots, A. B., & Dospassos, C. F. (1981). Studies of North-American Erora (Scudder) (Lepidoptera, Lycaenidae). *Journal of the New York Entomological Society*, *89*(4), 295–331.

Lovett, G. M., Arthur, M. A., Weathers, K. C., & Griffin, J. M. (2010). Long-term changes in Forest carbon and nitrogen cycling caused by an introduced Pest/pathogen complex. *Ecosystems*, *13*(8), 1188–1200. https://doi.org/10.1007/s10021-010-9381-y

Lovett, G. M., Canham, C. D., Arthur, M. A., Weathers, K. C., & Fitzhugh, R. D. (2006). Forest ecosystem responses to exotic pests and pathogens in eastern North America. *Bioscience*, *56*(5), 395–405. https://doi.org/10.1641/0006-3568(2006)056[0395:Fertep]2.0.Co;2

Marra, R. E., & LaMondia, J. A. (2020). First report of beech leaf disease, caused by the foliar nematode, Litylenchus crenatae mccannii, on American beech (*Fagus grandifolia*) in Connecticut. *Plant Disease*, *104*(9), 2527. https://doi.org/10.1094/pdis-02-20-0442-pdn

Martin, A. C., Zim, H. S., & Nelson, A. L. (1951). *American Wildlife & Plants: A guide to wildlife food habits: The use of trees, shrubs, weeds, and herbs by birds and mammals of the United States*. McGraw-Hill Book Copmany, Inc.

McAdam, S. A. M., Kane, C. N., Mercado Reyes, J. A., Cardoso, A. A., & Brodribb, T. J. (2022). An abrupt increase in foliage ABA levels on incipient leaf death occurs across vascular plants. *Plant Biology*, *24*(7), 1262–1271. https://doi.org/10.1111/plb.13404

McIntire, C. D. (2023). Physiological impacts of beech leaf disease across a gradient of symptom severity among understory American beech. *Frontiers in Forests and Global Change*, *6*(1146742), 1–9. https://doi.org/10.3389/ffgc.2023.1146742

Reed, S. E., Greifenhagen, S., Yu, Q., Hoke, A., Burke, D. J., Carta, L. K., Handoo, Z. A., Kantor, M. R., & Koch, J. (2020). Foliar nematode, Litylenchus crenatae ssp. mccannii, population dynamics in leaves and buds of beech leaf disease-affected trees in Canada and the US. *Forest Pathology*, *50*(3), e12599. https://doi.org/10.1111/efp.12599

Sack, L., Cowan, P. D., Jaikumar, N., & Holbrook, N. M. (2003). The 'hydrology' of leaves: co-ordination of structure and function in temperate woody species. *Plant Cell and Environment*, *26*(8), 1343–1356. https://doi.org/10.1046/j.0016-8025.2003.01058.x

Sack, L., & Scoffoni, C. (2012). Measurement of leaf hydraulic conductance and stomatal conductance and their responses to irradiance and dehydration using the evaporative flux method (EFM). *Jove-Journal of Visualized Experiments*, *70*(e4179), 1. https://doi.org/10.3791/4179

Sack, L., & Scoffoni, C. (2013). Leaf venation: Structure, function, development, evolution, ecology and applications in the past, present and future. *New Phytologist*, *198*(4), 983–1000. https://doi.org/10.1111/nph.12253

Sack, L., Scoffoni, C., John, G. P., Poorter, H., Mason, C. M., Mendez-Alonzo, R., & Donovan, L. A. (2013). How do leaf veins influence the worldwide leaf economic spectrum? Review and synthesis. *Journal of Experimental Botany*, *64*(13), 4053–4080. https://doi.org/10.1093/jxb/ert316

Sack, L., Scoffoni, C., McKown, A. D., Frole, K., Rawls, M., Havran, J. C., Tran, H., & Tran, T. (2012). Developmentally based scaling of leaf venation architecture explains global ecological patterns. *Nature Communications*, *3*, 837. https://doi.org/10.1038/ncomms1835

Sack, L., & Tyree, M. (2005). *Leaf hydraulics and its implications in plant structure and function* (pp. 93–114). Academic Press. https://doi.org/10.1016/B978-012088457-5/50007-1

Scoffoni, C., Sack, L., & Contributors, P. (2013). *Quantifying leaf vein traits. PrometheusWiki*. http://prometheuswiki.publish.csiro.au/tiki-pagehistory.php?page=Quantifying%20leaf%20vein%20traits&preview=15

Tsai, Y. H. E., & Manos, P. S. (2010). Host density drives the postglacial migration of the tree parasite, Epifagus virginiana. *Proceedings of the National Academy of Sciences of the United States of America*, *107*(39), 17035–17040. https://doi.org/10.1073/pnas.1006225107

Tyree, M. T., & Ewers, F. W. (1991). The hydraulic architecture of trees and other woody plants. *New Phytologist*, *119*(3), 345–360. https://doi.org/10.1111/j.1469-8137.1991.tb00035.x

Vieira, P., Kantor, M. R., Jansen, A., Handoo, Z. A., & Eisenback, J. D. (2023). Cellular insights of beech leaf disease reveal abnormal ectopic cell division of symptomatic interveinal leaf areas. *PLoS One*, *18*(10), e0292588. https://doi.org/10.1371/journal.pone.0292588

Volk, D. R., Hausman, C. E., & Martin, D. K. (2019). *Beech leaf disease seasonal symptom progression*. Division of Natural Resources, Cleveland Metroparks.

Zhang, M., Gao, H. R., Chen, S., Wang, X. C., Mo, W. Y., Yang, X., Wang, X., Wang, Z. B., & Wang, R. L. (2022). Linkages between stomatal density and minor leaf vein density across different altitudes and growth forms. *Frontiers in Plant Science*, *13*, 1064344. https://doi.org/10.3389/fpls.2022.1064344

SUPPORTING INFORMATION

Additional supporting information can be found online in the Supporting Information section at the end of this article.

How to cite this article: Fletcher, L. R., Borsuk, A. M., Fanton, A. C., Johnson, K. M., Richburg, J., Zailaa, J., & Brodersen, C. R. (2024). Anatomical and physiological consequences of beech leaf disease in *Fagus grandifolia* L. *Forest Pathology*, *54*, e12842. https://doi.org/10.1111/efp.12842